Mixed projection- and density-based topology optimization with applications to structural assemblies

Nicolo Pollini and Oded Amir

Faculty of Civil & Environmental Eng., Technion – Israel Institute of Technology

TOP webinar #4, August 27 2020

The paper in SAMO

Structural and Multidisciplinary Optimization
https://doi.org/10.1007/s00158-019-02390-9

RESEARCH PAPER

Check for updates

Mixed projection- and density-based topology optimization with applications to structural assemblies

Nicolò Pollini[1] · Oded Amir[2]

Received: 10 June 2019 / Revised: 6 August 2019 / Accepted: 13 August 2019

Motivation: optimize a design and its partitioning

Task: redesign an engine support rib for AM

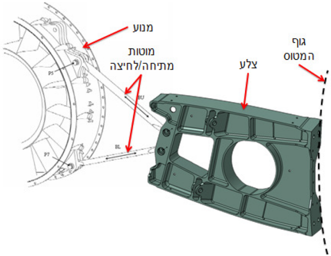

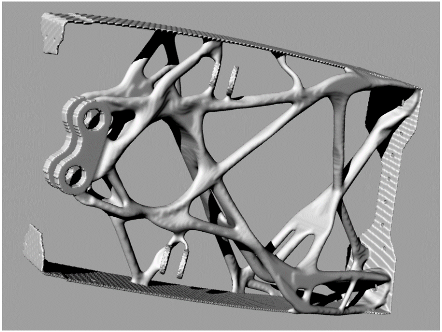

Challenges:

- Rib is bigger than AM facility $\rightarrow$ print in parts and weld
- Welding of printed parts: mostly unknown territory
- What are the constraints??? material? geometry?

FOCUS ON THE CONCEPTUAL GEOMETRIC PROBLEM

Motivation: optimize a design and its partitioning

Main idea

Optimizing the design and later searching for the best partition may result in **sub-optimal**, or even **infeasible** results with respect to the manufacturing scenario

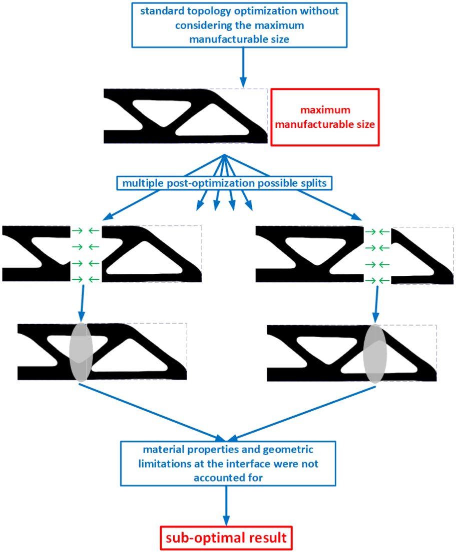

Optimizing the assembly 'cut'

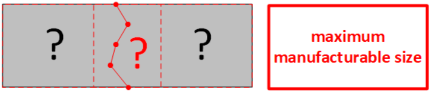

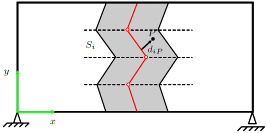

$$
\begin{aligned}
\underset{\boldsymbol{\rho},\mathbf{x}}{\text{minimize}} :&\quad f(\boldsymbol{\rho},\mathbf{x}) \\
\text{subject to} :&\quad g_k(\boldsymbol{\rho},\mathbf{x}) \le 0, \qquad k = 0,\dots,m \\
:&\quad 0 \le \rho_i \le 1, \qquad i = 1,\dots,N_{ele} \\
:&\quad x_{lb} \le x_j \le x_{ub}, \qquad j = 1,\dots,N_{node} \\
\text{with} :&\quad \mathbf{K}(\boldsymbol{\rho},\mathbf{x})\,\mathbf{u} = \mathbf{f}
\end{aligned}
$$

- $\boldsymbol{\rho}$ is the common density-based design field
- $\mathbf{x}$ are geometric coordinates of the cut
- Constraints g_k contain the controls over the design near the cut, and a standard total volume constraint

Evolution of the design parametrization

The problem statement is a **shape** and (freeform) **topology** optimization coupled by **geometric projection**

How to optimally embed a **discrete object** within an **otherwise freeform** continuum domain?

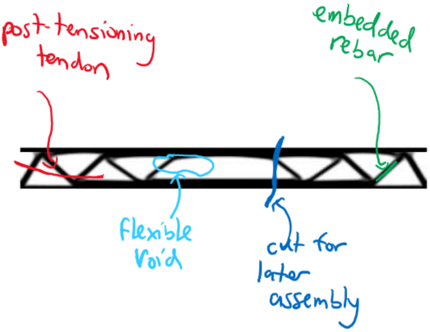

Discrete-continuum coupling (1)

Coupling a ground structure of rebars to continuum concrete: a rebar-concrete filter [Amir, 2013]

$$\tilde{x}_i = x_i \frac{1}{N_{ij}} \sum_{j \in N_i} (\bar{x}_j)^{p_E}$$

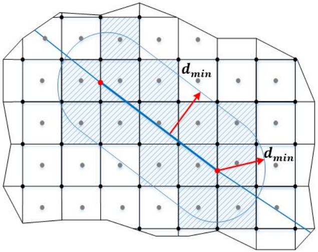

Definition of neighborhood

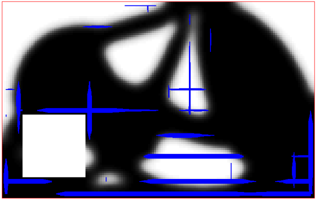

Without filter

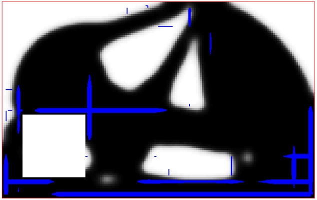

With filter

Discrete-continuum coupling (2)

Coupling a post-tensioning tendon to continuum concrete: a tendon-to-concrete filter [Amir and Shakour, 2018]

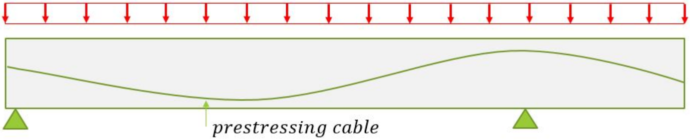

cable profile determined according to bending moments

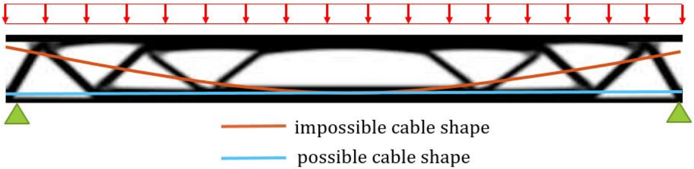

optimized beam did not consider the prestressed tendon

The application in post-tensioned concrete

Concrete distribution is determined by filter and projection operations:

1. Density filter
   [Bruns and Tortorelli, 2001, Bourdin, 2001] :

$$\widetilde{\rho}_i = \frac{\sum_{j \in N_i} w(\mathbf{x}_j) v_j \rho_j}{\sum_{j \in N_i} w(\mathbf{x}_j) v_j}$$

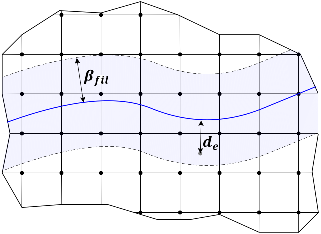

2. Tendon-to-concrete filter:

$$\hat{\rho}_i = \widetilde{\rho}_i + (1 - \widetilde{\rho}_i) e^{-\frac{1}{2}\left(\frac{d_i}{\beta_{fil}}\right)^{\mu}}$$

3. Heaviside projections – 'robust' approach
   [Guest et al., 2004, Wang et al., 2011, Lazarov et al., 2016] :

$$\overline{\rho}_i^{ero} = \frac{\tanh(\beta_{HS}\eta_{ero}) + \tanh(\beta_{HS}(\hat{\rho}_i - \eta_{ero}))}{\tanh(\beta_{HS}\eta_{ero}) + \tanh(\beta_{HS}(1 - \eta_{ero}))}$$

$$\overline{\rho}_i^{dil} = \frac{\tanh(\beta_{HS}\eta_{dil}) + \tanh(\beta_{HS}(\hat{\rho}_i - \eta_{dil}))}{\tanh(\beta_{HS}\eta_{dil}) + \tanh(\beta_{HS}(1 - \eta_{dil}))}$$

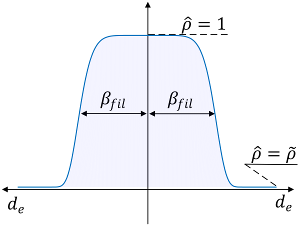

The application in post-tensioned concrete

Line object (tendon) and freeform continuum (concrete) are optimized concurrently with a geometric projection coupling them

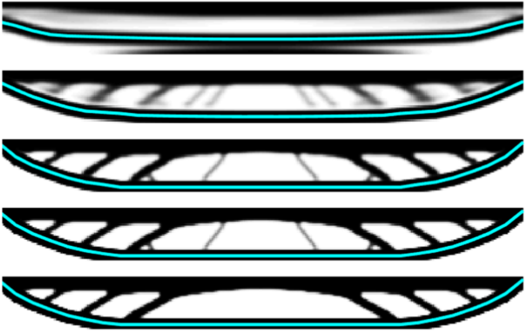

Manufacturing by 3D printing

Collaboration with Gieljan Vantyghem & Wouter de Corte, Ghent U.

...Back to our problem statement

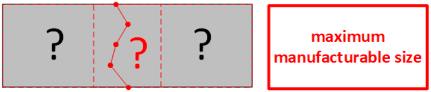

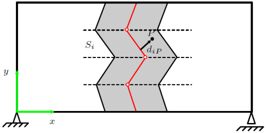

$$
\begin{aligned}
\underset{\boldsymbol{\rho},\mathbf{x}}{\text{minimize}} &: \quad f(\boldsymbol{\rho}, \mathbf{x}) \\
\text{subject to} &: \quad g_k(\boldsymbol{\rho}, \mathbf{x}) \leq 0, \quad k = 0, ..., m \\
&: \quad 0 \leq \rho_i \leq 1, \quad i = 1, ..., N_{ele} \\
&: \quad x_{lb} \leq x_j \leq x_{ub}, \quad j = 1, ..., N_{node} \\
\text{with} &: \quad \mathbf{K}(\boldsymbol{\rho}, \mathbf{x})\, \mathbf{u} = \mathbf{f}
\end{aligned}
$$

- $\boldsymbol{\rho}$ is the common density-based design field
- $\mathbf{x}$ are geometric coordinates of the cut
- Constraints g_k contain the controls over the design near the cut, and a standard total volume constraint

Common density-based building blocks

Three-field density representation, $\boldsymbol{\rho} \rightarrow \tilde{\boldsymbol{\rho}} \rightarrow \bar{\boldsymbol{\rho}}$

1. Density filter [Bruns and Tortorelli, 2001, Bourdin, 2001]:

$$\tilde{\rho}_i = \frac{\sum_{j \in N_i} w(\Delta \mathbf{x}_{ij}) \rho_j}{\sum_{j \in N_i} w(\Delta \mathbf{x}_{ij})}$$

2. Smooth Heaviside projections

[Guest et al., 2004, Wang et al., 2011, Lazarov et al., 2016]:

$$\bar{\rho}_i^{ero} = \frac{tanh\left(\beta_{HS}\eta_{ero}\right) + tanh\left(\beta_{HS}(\tilde{\rho}_i - \eta_{ero})\right)}{tanh\left(\beta_{HS}\eta_{ero}\right) + tanh\left(\beta_{HS}(1 - \eta_{ero})\right)},$$

$$\bar{\rho}_i^{int} = \frac{tanh\left(\beta_{HS}\eta_{int}\right) + tanh\left(\beta_{HS}(\tilde{\rho}_i - \eta_{int})\right)}{tanh\left(\beta_{HS}\eta_{int}\right) + tanh\left(\beta_{HS}(1 - \eta_{int})\right)},$$

$$\bar{\rho}_i^{dil} = \frac{tanh\left(\beta_{HS}\eta_{dil}\right) + tanh\left(\beta_{HS}(\tilde{\rho}_i - \eta_{dil})\right)}{tanh\left(\beta_{HS}\eta_{dil}\right) + tanh\left(\beta_{HS}(1 - \eta_{dil})\right)},$$

with e.g. $\eta_{ero} = 0.6,\ \eta_{int} = 0.5,\ \eta_{dil} = 0.4$

Line-to-continuum projection

Projection achieved using Super-Gaussian functions:

$$\phi_{i,j} = e^{-\frac{1}{2}\left(\frac{d_{i,j}^2}{\beta_\phi^2}\right)^{\mu_\phi}}, \text{ for } j = 1, \ldots, N_{ele}$$

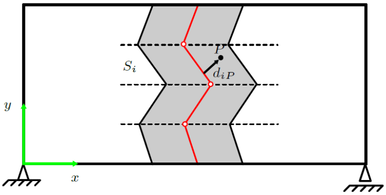

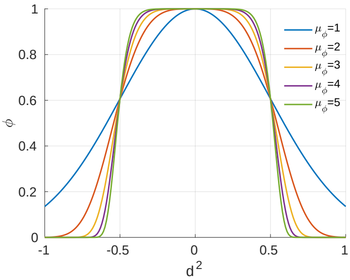

A point near two cuts

Naively summing the projection functions is not suitable:

$$\phi_i = e^{-\frac{1}{2}\left(\frac{d_{1,i}^2}{\beta_\phi^2}\right)^{\mu_\phi}} + e^{-\frac{1}{2}\left(\frac{d_{2,i}^2}{\beta_\phi^2}\right)^{\mu_\phi}}, \text{ for } i = 1, \ldots, N_{ele}$$

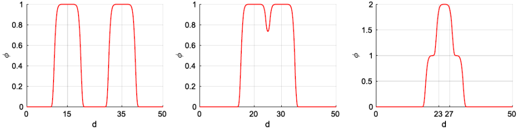

(a) $x_{01} = 15$ $x_{02} = 35$. (b) $x_{01} = 20$ $x_{02} = 30$. (c) $x_{01} = 23$ $x_{02} = 27$.

Use a differentiable minimum distance with large q:

$$\bar{d}_i^2 = d_{max}^2 - \frac{\left(d_{max}^2 - d_{1,i}^2\right)^{q+1} + \left(d_{max}^2 - d_{2,i}^2\right)^{q+1}}{\left(d_{max}^2 - d_{1,i}^2\right)^{q} + \left(d_{max}^2 - d_{2,i}^2\right)^{q}}$$

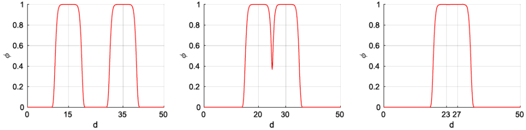

(a) $x_{01} = 15$ $x_{02} = 35$. (b) $x_{01} = 20$ $x_{02} = 30$. (c) $x_{01} = 23$ $x_{02} = 27$.

Avoiding sharp distance fields

The point-to-segment distance field is filtered to avoid sharp transitions:

$$\tilde{d}_i^2 = \frac{\sum_{j \in N_i} w(\Delta \mathbf{x}_{ij}) \bar{d}_j^2}{\sum_{j \in N_i} w(x_j)}$$

(a) Graphic representation of the projection profile (b) $\phi(\bar{d})$ - distance field not filtered (c) $\phi(\tilde{d})$ - filtered distance field

The filtered distance eventually enters the Super-Gaussian projection.

Basic components of problem formulation

Objective is minimum compliance of eroded design [Lazarov et al., 2016]:

$$f(\boldsymbol{\rho}, \mathbf{x}) = \mathbf{f}^T \, \mathbf{u}(\bar{\boldsymbol{\rho}}^{ero}, \mathbf{x}) \qquad \mathbf{K}(\bar{\boldsymbol{\rho}}^{ero}, \mathbf{x}) \, \mathbf{u} = \mathbf{f}$$

Modified SIMP interpolation scheme [Sigmund and Torquato, 1997]:

$$E_i = E_{min} + (E_{max} - E_{min}) \, (\bar{\rho}_i^{ero})^{p_E}$$

Volume constraint on the full structural domain:

$$g_0(\boldsymbol{\rho}) = \frac{\sum_{i=1}^{N_{ele}} \bar{\rho}_i^{dil} v_i}{\sum_{i=1}^{N_{ele}} v_i} - g_{0,dil}^* \leq 0$$

Slope constraint to regularize the cut:

$$g_3(\mathbf{x}) = \frac{1}{\Delta x_{max}^2} \left(\sum_{i=1}^{N_{node}-1} \left(\Delta x_i^2\right)^p \right)^{\frac{1}{p}} - 1 \leq 0$$

Sensitivity analysis

Lots of chain rules... details are in the paper

MATLAB code can be provided upon request

Control over projected region: volume

1. Maximum volume in the region of the cut (e.g. limit welding energy)

$$g_1(\boldsymbol{\rho}, \mathbf{x}) = \frac{\sum_{i=1}^{N_{ele}} \bar{\rho}_i^{dil} v_i \, \phi_i(\mathbf{x})}{\sum_{i=1}^{N_{ele}} v_i \, \phi_i(\mathbf{x})} - g_{1,dil}^* \leq 0$$

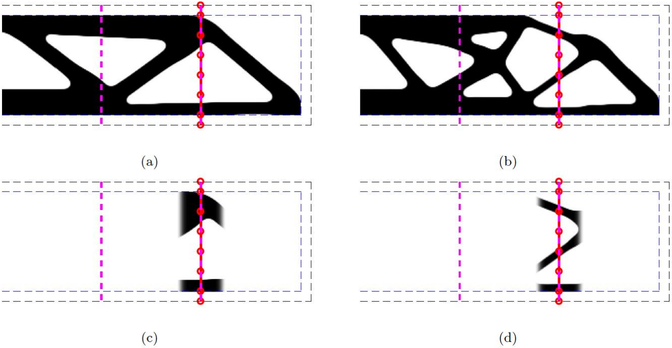

Volume fraction is limited to 25% in the region of the cut

compliance 194.1 $\rightarrow$ 202.1

Control over projected region: stiffness

2. Assign a Young's modulus equal to E_ϕ to the elements in the region of the cut:

$$E_i = E_{min} + (E_{max} - (E_{max} - E_\phi)\,\phi_i - E_{min})\,\bar{\rho}_{i,ero}^{p_E}$$

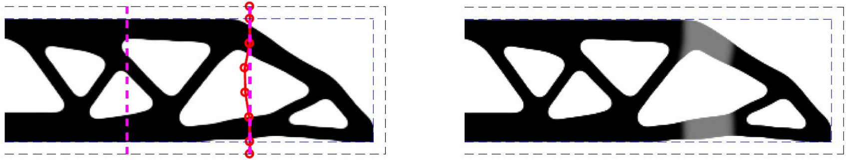

with $E_\phi = 0.5E_{max}$, compliance 194.1 $\rightarrow$ 207.1

- Can be extended to other material properties, e.g. stress

Control over projected region: max thickness

3. Maximum length scale [Guest, 2009, Wu et al., 2018] in the region of the cut (e.g. limit thickness of connected members)

$$g_2(\hat{\rho}, \mathbf{x}) = \left(\frac{\sum_{i=1}^{N_{ele}} \hat{\rho}_i^p \phi_i}{\sum_{i=1}^{N_{ele}} \phi_i} \right)^{1/p} - \alpha \leq 0$$

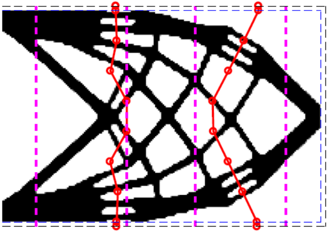

(a)

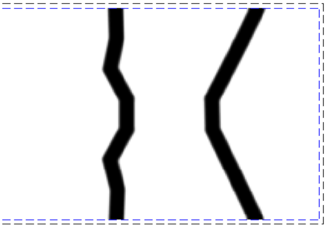

(b)

compliance 38.92 $\rightarrow$ 44.84

Control over projected region: max thickness

3. Maximum length scale [Guest, 2009, Wu et al., 2018] in the region of the cut (e.g. limit thickness of connected members)

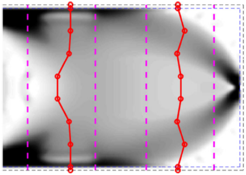

(a) Iter = 10

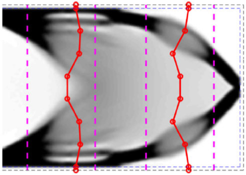

(b) Iter = 25

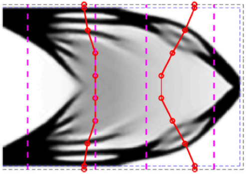

(c) Iter = 50

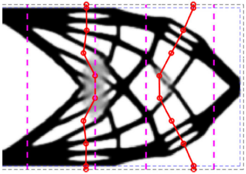

(d) Iter = 100

Control over projected region: max thickness

3. Maximum length scale [Guest, 2009, Wu et al., 2018] in the region of the cut (e.g. limit thickness of connected members)

$$g_2(\hat{\rho}, \mathbf{x}) = \left(\frac{\sum_{i=1}^{N_{ele}} \hat{\rho}_i^p \phi_i}{\sum_{i=1}^{N_{ele}} \phi_i} \right)^{1/p} - \alpha \leq 0$$

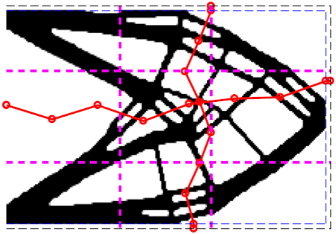

(a)

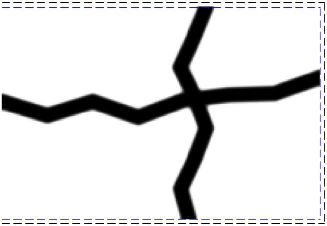

(b)

compliance 38.92 $\rightarrow$ 47.38

Control over projected region: filter radius

4. Spatial variation of length scale in the region of the cut

[Amir and Lazarov, 2018]

$$\bar{r}_{min}(\phi_i) = r_{min}(1 + \gamma\,\phi_i)$$

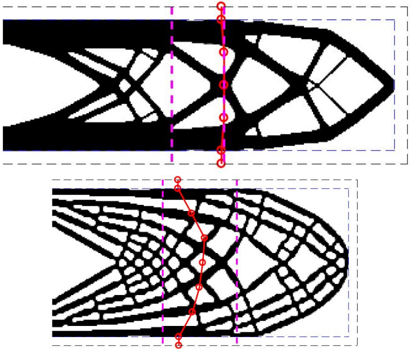

- Find the region in which to increase either the minimum or maximum size
- Both cases lead to fewer and thicker members at assembly interface

Some related work

- Embedding of pre-designed polygonal objects
  [Qian and Ananthasuresh, 2004]
- Integrated optimization of component layout and topology
  [Xia et al., 2013]
- Material density and level sets for embedding movable holes
  [Kang and Wang, 2013]
- Explicit topology optimization with multiple embedding components [Zhang et al., 2015]
- Integrated optimization of discrete thermal conductors and solid material [Li et al., 2017]
- A combined parametric shape optimization and ersatz material approach [Wein and Stingl, 2018]
- **Thorough discussion in review by Wein, Dunning & Norato**

Summary

- Presented a **coupled parametrization** for concurrent design of a structure, its **partition into parts** and the **assembly interface**
- Control over the region of the interface: minimum and maximum sizes, material properties, material quantity, shape of the cut, etc.
- Many possibilities for coupling density and projection: get the **best of both worlds???**

Density-based

+ Most design space freedom
+ Smooth and well-behaved
– Limited geometric control

Geometric projection

+ Explicit, precise geometric control
– Restricted design freedom
– Could be highly nonlinear
* a.k.a. feature-mapping

Questions?

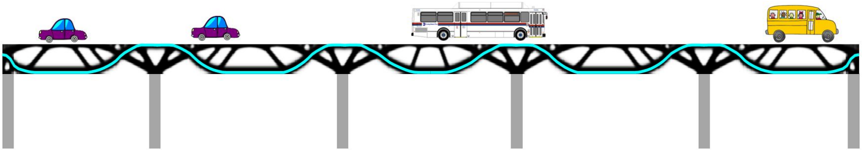

References I

Amir, O. (2013).
A topology optimization procedure for reinforced concrete structures.
Computers & Structures, 114-115:46–58.

Amir, O. and Lazarov, B. S. (2018).
Achieving stress-constrained topological design via length scale control.
Structural and Multidisciplinary Optimization, pages 1–19.

Amir, O. and Shakour, E. (2018).
Simultaneous shape and topology optimization of prestressed concrete beams.
Structural and Multidisciplinary Optimization, 57(5):1831–1843.

Bourdin, B. (2001).
Filters in topology optimization.
International Journal for Numerical Methods in Engineering, 50:2143–2158.

Bruns, T. E. and Tortorelli, D. A. (2001).
Topology optimization of non-linear elastic structures and compliant mechanisms.
Computer Methods in Applied Mechanics and Engineering, 190:3443–3459.

Guest, J. K. (2009).
Imposing maximum length scale in topology optimization.
Structural and Multidisciplinary Optimization, 37(5):463–473.

Guest, J. K., Prévost, J. H., and Belytschko, T. (2004).
Achieving minimum length scale in topology optimization using nodal design variables and projection functions.
International Journal for Numerical Methods in Engineering, 61:238–254.

References II

Kang, Z. and Wang, Y. (2013).
Integrated topology optimization with embedded movable holes based on combined description by material density and level sets.
Computer Methods in Applied Mechanics and Engineering.

Lazarov, B. S., Wang, F., and Sigmund, O. (2016).
Length scale and manufacturability in density-based topology optimization.
Archive of Applied Mechanics, 86(1-2):189–218.

Li, Y., Wei, P., and Ma, H. (2017).
Integrated optimization of heat-transfer systems consisting of discrete thermal conductors and solid material.
International Journal of Heat and Mass Transfer.

Qian, Z. and Ananthasuresh, G. K. (2004).
Optimal embedding of rigid objects in the topology design of structures.
Mechanics Based Design of Structures and Machines, 32(2):165–193.

Sigmund, O. and Torquato, S. (1997).
Design of materials with extreme thermal expansion using a three-phase topology optimization method.
Journal of the Mechanics and Physics of Solids, 45(6):1037–1067.

Wang, F., Lazarov, B. S., and Sigmund, O. (2011).
On projection methods, convergence and robust formulations in topology optimization.
Structural and Multidisciplinary Optimization, 43:767–784.

Wein, F. and Stingl, M. (2018).
A combined parametric shape optimization and ersatz material approach.
Structural and Multidisciplinary Optimization, 57(3):1297–1315.

References III

Wu, J., Aage, N., Westermann, R., and Sigmund, O. (2018).
Infill optimization for additive manufacturing: approaching bone-like porous structures.
IEEE transactions on visualization and computer graphics, 24(2):1127–1140.

Xia, L., Zhu, J., Zhang, W., and Breitkopf, P. (2013).
An implicit model for the integrated optimization of component layout and structure topology.
Computer Methods in Applied Mechanics and Engineering.

Zhang, W., Zhong, W., and Guo, X. (2015).
Explicit layout control in optimal design of structural systems with multiple embedding components.
Computer Methods in Applied Mechanics and Engineering.